

Resolving plant transformation recalcitrance by Agrobacterium-mediated protein translocation Gariboldi. I.

Citation

Gariboldi, I. (2025, October 28). Resolving plant transformation recalcitrance by Agrobacterium-mediated protein translocation. Retrieved from https://hdl.handle.net/1887/4281769

Version: Publisher's Version

Licence agreement concerning inclusion of doctoral

License: thesis in the Institutional Repository of the University

of Leiden

Downloaded from: https://hdl.handle.net/1887/4281769

Note: To cite this publication please use the final published version (if applicable).

Chapter 2

A generic detection system for *Agrobacterium*-mediated DNA and protein translocation to plant cells

Ivo Gariboldi¹, Jaap Tromp¹, Koen van Oostrom¹, Anton Rotteveel¹, Maarten Stuiver², Remko Offringa^{1,*}

¹ Plant Developmental Genetics, Institute of Biology Leiden, Leiden University, Sylviusweg 72, 2333 BE, Leiden, The Netherlands

 $^{^2}$ Research Technology and Disease Control, BASF Innovation Center, Technologiepark-Zwijnaarde 101, 9052 Ghent, Belgium

^{*} Author for correspondence: r.offringa@biology.leidenuniv.nl

Abstract

The use of *Agrobacterium tumefaciens* (Agrobacterium) for plant transformation has long focused on stable T-DNA integration or transient expression, where stable T-DNA integration was generally selected for by co-expressing an antibiotic or herbicide resistance gene. The finding that Agrobacterium also translocates Vir proteins, or heterologous proteins fused to these Vir proteins, to host plant cells has provided an interesting additional tool for the reprogramming of plant cells or the editing of their genomes. In this chapter, the split-GFP system was optimized for sensitive visualization of translocation of GFP₁₁-tagged proteins of interest to plant cells. In addition, a split-Cherry system was tested to detect the simultaneous translocation of a Cherry₁₁-tagged protein of interest. Unfortunately, the split-Cherry system was not suitable for the detection of protein translocation. Instead, we successfully used the *Cherry* reporter in combination with the optimized split-GFP system to visualize simultaneous T-DNA transfer and protein translocation in leaves of *Nicotiana tabacum*, *Nicotiana benthamiana*, *Solanum lycopersicum*, *Capsicum annuum*, *Brassica napus* and suspension cells of *Arabidopsis thaliana*.

Introduction

Plants are commonly genetically modified for experimental or breeding purposes using the natural DNA transfer system of the soil-borne phytopathogen *Agrobacterium tumefaciens* (Agrobacterium). It has the ability to transfer a part of its DNA (transfer DNA or T-DNA) together with Virulence proteins (Vir proteins) to the host plant cell. The T-DNA originates from the tumor-inducing plasmid (Ti plasmid) and contains all the genes necessary to cause tumor growth on the plant and to make these tumor cells produce compounds beneficial for the bacterium. The Vir proteins aid in the process of transformation by, among others, forming the type IV secretion system (T4SS) pilus and guiding the T-DNA strand towards the plant cell nucleus (Nester, 2015).

For these guiding Vir proteins, such as VirE2 and VirF, it was shown that they are translocated together with the T-DNA by the T4SS to plant cells and that a positively charged C-terminal signal sequence in these proteins is required and sufficient for translocation. Heterologous proteins C-terminally fused to this signal sequence can be introduced into plant cells by Agrobacterium-mediated protein translocation (AMPT) (Vergunst et al., 2000, 2005). To prove transfer of heterologous proteins by AMPT to plant cells, the Cre recombinase was fused to the C-terminal domain of VirE2 or VirF and translocation was tested using a transgenic Arabidopsis thaliana (Arabidopsis) line containing a lox-flanked DNA segment. This segment separated the coding region of the neomycin phosphotransferase II (nptII) gene from the promoter, thereby preventing its expression. Successful transfer of the Cre fusion protein led to excision of the segment and thus to restoration of nptII expression. This expression could be detected by the appearance of kanamycin resistant calli, thereby proving that Agrobacterium was capable of protein translocation (Vergunst et al., 2000). Although a robust system, it could only report AMPT in an indirect manner. The green fluorescent protein (GFP), often used for visualization of expression, cannot be translocated using AMPT. To directly visualize AMPT, the split-GFP system was adopted to detect the translocation of VirE2 into Nicotiana tabacum (Sakalis et al., 2014). The general concept of the split-GFP system is that GFP is split into two non-fluorescent parts, a larger fragment comprising amino acids 1-214 (GFP₁₋₁₀, detector) and a smaller fragment comprising amino acids 214-230 (GFP₁₁, tag), that are able to self-assemble into a fluorescent GFP molecule (Ghosh et al., 2000b). For this purpose, GFP has been optimized to prevent misfolding when the GFP₁₁ tag is expressed as fusion with other proteins. This so called superfolder GFP, hereafter referred to as GFP, has increased solubility, which increases the fluorescence in living cells and the extraction efficiency of the protein (Pédelacq et al., 2006). In contrast to many other protein tagging techniques, the split-GFP system is highly suitable for *in vivo* work. In the first approaches to visualize AMPT using split-GFP, plants that stably express the GFP₁₋₁₀ were co-cultivated with Agrobacterium transferring a fusion protein VirE2 N-terminally tagged with GFP₁₁ (Sakalis et al., 2014). The system was further optimized by expressing the GFP₁₋₁₀ from a T-DNA that was co-transferred with the translocated GFP₁₁-tagged protein of interest (POI), enabling direct visualization of AMPT in wild-type plants without the need for *a priori* transformation (Khan, 2017).

The above system had the disadvantage that the sensitivity of detecting AMPT was limited when compared to the transient expression of the GFP₁₁-tagged POI from a T-DNA (Khan, 2017), suggesting that many AMPT events were left undetected. Moreover, our previous AMPT data suggested that for many plant genotypes that have been reported to be recalcitrant to AMT, both T-DNA transfer and AMPT could be detected (Khan, 2017), suggesting that the main bottle neck is the regeneration of the transformed cells. Previously, it has been reported that the simultaneous expression of the transcription factors BABY BOOM (BBM) and WUSCHEL (WUS) in plant cells significantly enhances the frequency of transformation and regeneration in numerous previously difficult to transform crop species and tissues, such as maize (Zea mays) immature embryos and callus, sorghum (Sorghum bicolor) immature embryos, sugarcane (Saccharum officinarum) callus and rice (Oryza sativa ssp indica) callus (Lowe et al., 2016). A major disadvantage of this system is that it requires removal of these genes during the process of regeneration, because sustained expression of these transcription factors interfere with plant development. We therefore tested whether simultaneous introduction of the BBM and WUS proteins via AMPT would lead to enhanced regeneration without the need to remove the genes. As this required the detection of translocation of

two POIs, we adopted the split-variant of *super folder* Cherry 2 (hereafter referred to as split-Cherry), which has previously only been tested in animal cells (Feng et al., 2017; Kamiyama et al., 2016b), into our AMPT system for the detection of the second POI.

In this chapter we describe several approaches to optimize the detection of AMPT for the simultaneous translocation of two POIs. We show that the detection of AMPT by the split-GFP system can be enhanced by optimization of the $GFP_{11}:POI:\Delta virF$ coding region for expression in Agrobacterium and by a seventimes multimerization of the GFP_{11} tag. Unfortunately, it appeared impossible to detect AMPT using the split-Cherry system, either due to insufficient sensitivity of the system or because the Cherry₁₁ tag prohibited AMPT. Instead, we successfully used the *Cherry* reporter in combination with the improved split-GFP system, to detect simultaneous AMT and AMPT in different tissues of various plant species.

Results

Optimized detection of AMPT in tobacco leaf cells

The previously observed fluorescence by confocal microscopy after AMPT using the split-GFP system (split-GFP^{mk}) using GFP₁₁ protein translocation and a GFP₁₋₁₀T-DNA transfer vector was relatively weak compared to *p35S* driven transient expression of full length GFP following DNA transfer (Khan, 2017). High laser power was required to be able to clearly visualize the signal by confocal microscopy, causing unwanted tissue damage and rapid bleaching of the fluorescent signal. One of the reasons for the weak signal could be that the coding regions in the split-GFP system were not optimized for the species-specific codon usage. We therefore optimized the *GFP*₁₁ sequence as used in the coding region of GFP₁₁:POI:ΔVirF (Appendix 1a) and the sequence of the POI, BBM (Appendix 1e) for expression in Agrobacterium. At the same time, the *NLS* and *GFP* sequences forming the *NLS:GFP*₁₋₁₀ coding region on the T-DNA vector were optimized for expression in plants (Appendix 1b). An Agrobacterium strain containing the resulting vectors *pvirF::GFP*₁₁:BBM:Δ*virF* and *p35S::NLS:GFP*₁₋₁₀::tNOS was infiltrated into *Nicotiana tabacum* (tobacco) leaves. At 4 days post infiltration (dpi) nuclear fluorescent GFP signal was observed,

indicating that AMPT was successful. The fluorescence intensity of the nuclear signal was compared to that in leaves infiltrated with an Agrobacterium strain translocating a non-optimized GFP₁₁:BBM:ΔVirF fusion protein (Khan, 2017) together with the plant optimized p35S::NLS:GFP₁₋₁₀::tNOS T-DNA construct. With the Agrobacterium optimized fusion protein, significantly more positive nuclei were detected, and in those nuclei the fluorescent signal was on average 2-fold stronger compared to fluorescent nuclei obtained following AMPT of the non-optimized protein (Fig. 1A, B). These data suggest that codon optimization does lead to higher expression in Agrobacterium and thus to more AMPT events, resulting in a stronger signal in plants. Therefore, all the constructs used in subsequent experiments were codon optimized for either plant or bacterial expression. To further increase detection of the fluorescent signal, the GFP₁₁ tag was multimerized seven times, resulting in the pvirF::GFP₁₁x7:BBM:ΔvirF construct. Multimerization of the GFP₁₁ tag should provide more binding places for the abundantly overexpressed GFP₁₋₁₀ sensor, which has been reported to lead to a significant enhancement of the signal (Kamiyama et al., 2016b; Park et al., 2017). In our experiments, more fluorescence positive nuclei were observed with the GFP₁₁x7:BBM:ΔVirF fusion proteins and the average fluorescence intensity per nucleus was 2-fold higher compared to that with the single GFP₁₁-tagged codon optimized fusion protein (Fig. 1A, B).

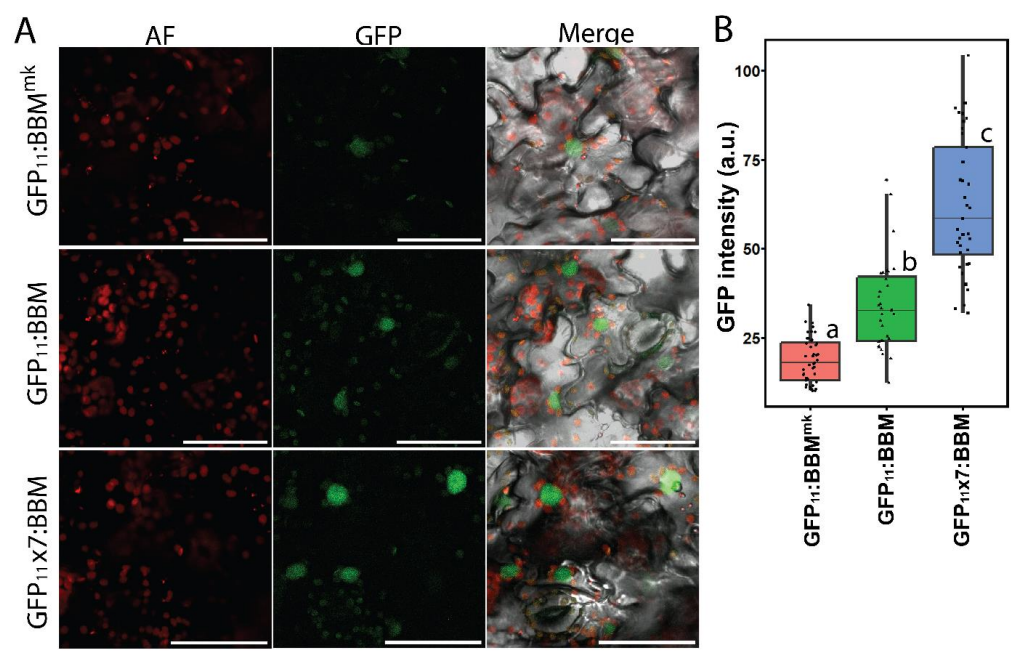


Figure 1. Enhanced detection of AMPT of BBM fusions by modifying the split GFP system. (A) Confocal microscopy images showing GFP fluorescence observed 4 dpi in 4-weeks old tobacco leaf epidermis cells after AMPT using split-GFP system variants: the non-optimized split-GFP^{mk} (p35S::NLS:GFP₁₋₁₀mk::tNOS + pvirF::GFP₁₁mk:BBM^{mk}:\(\Delta\)virF), the codon optimized split-GFP (p35S::NLS:GFP₁₋₁₀::tNOS + pvirF::GFP₁₁:BBM:ΔvirF) and the codon optimized split-GFP with 7 tandem GFP₁₁ repeats ($p355::NLS:GFP_{1-10}::tNOS + pvirF::GFP_{11}x7:BBM:\Delta virF$). The GFP₁₁-BBM-ΔVirF was expressed from the protein translocation vector and NLS-GFP₁₋₁₀ was expressed from a T-DNA in the plant cell. Scale bars indicate 50 μm. AF: autofluorescence. (B) Quantification of the intensity of the nuclear GFP signal in tobacco mesophyll cells after AMPT of a non-optimized fusion protein (GFP₁₁:BBM^{mk}), a bacterial codon-optimized fusion protein (GFP₁₁:BBM) and a bacterial codon optimized fusion protein with GFP₁₁ multimerization (GFP₁₁x7:BBM). For each treatment 36 nuclei were measured in images taken from the 3th, 4th and 5th leaf of 12 tobacco plants. The dots indicate the fluorescence intensity per nucleus. Different letters indicate statistically significant differences (p < 0.001) as determined by one-way analysis of variance (ANOVA) with Tukey's honest significant difference post hoc test.

Testing the split-Cherry reporter for AMPT to plant cells

Our aim was to use AMPT for the simultaneous translocation of the regeneration enhancing transcription factors BBM and WUS. This required the use of a second split-fluorophore system to be able to detect AMPT of both proteins. Previously, a split-fluorophore system was reported in animal systems using Cherry (Nguyen et

al., 2013) and it was shown that it can be simultaneously used with the split-GFP system as the fluorophore fragments are not able to cross-associate (Feng et al., 2017; Kamiyama et al., 2016a). As a first approach to test the use of split-Cherry in plants, the *NLS:GFP* coding region on a positive control T-DNA construct was replaced by that of *NLS:Cherry* (Fig. 2A, Appendix 1c), codon optimized for plant expression (Puigbò et al., 2007) and containing an intron at the same relative position as in GFP (Haseloff et al., 1997) (Appendix 1b). Clear Cherry fluorescence, both nuclear and cytoplasmic, was observed in epidermis cells of 4-weeks old tobacco leaves at 4 dpi with an Agrobacterium strain containing the *p35S::NLS:Cherry::tNOS* construct, indicating that Cherry is a suitable reporter in plant cells (Fig. 2B).

The next step was to test the reconstitution of the split-Cherry parts in plant cells. Therefore, the *GFP*₁₋₁₀ coding region on the T-DNA transfer construct of the split-GFP system was replaced by the *Cherry*₁₋₁₀ sequence. On the same T-DNA the *Cherry*₁₁:*WUS*:Δ*virF* coding region was cloned behind a second *35S* promoter (Fig. 2C). Following infiltration of tobacco leaves with an Agrobacterium strain containing the resulting construct, clear nuclear and cytosolic Cherry fluorescence could be detected at 4 dpi in leaf epidermis cells (Fig. 2D). These results show that also the codon optimized split-Cherry system is functional in plants, at least when both components are expressed from a single T-DNA.

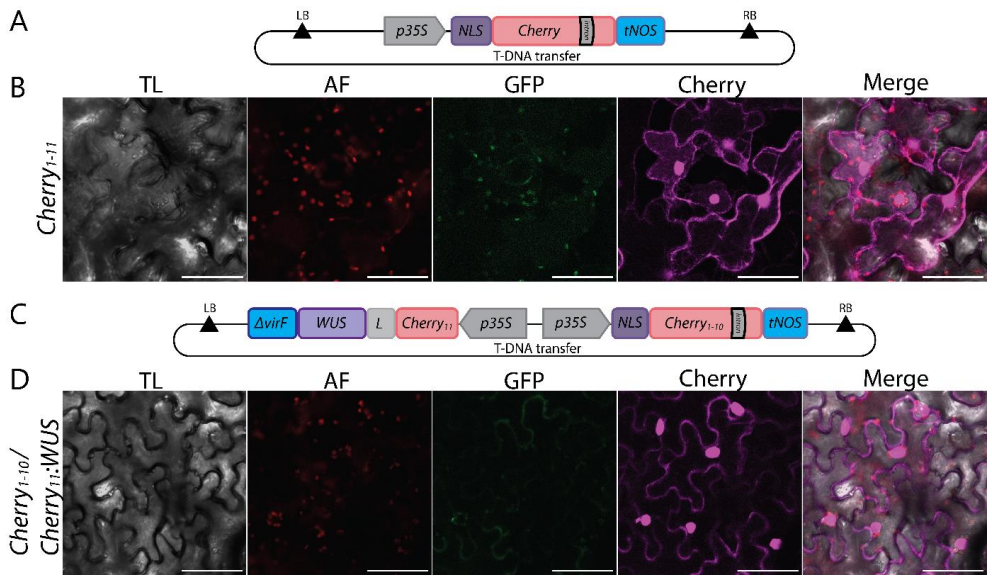


Figure 2. The Cherry fluorophore-based split system can be used as a reporter in plant cells. (A, C) T-DNA constructs *p355::NLS:Cherry::tNOS* (A) and *p355::NLS:Cherry1-10::tNOS/p355::Cherry1:WUS:ΔvirF::tNOS* (C) to test the use of the split-Cherry system in plant cells. (B, D) Confocal microscopy images showing Cherry fluorescence at 4 dpi in leaf epidermis cells of 4-weeks old tobacco plants after AMT of a T-DNA expressing full-length Cherry (A, B) or the split-Cherry system (C,D). Scale bars indicate 50 μm. Abbreviations: TL, transmitted light; AF, autofluorescence; p35S, *Cauliflower Mosaic Virus 35S* promoter; NLS, nuclear localization signal; tNOS, nopaline synthase transcriptional terminator; L, Linker sequence coding for 9 amino acids connecting the fluorophore11 tag and the protein of interest (POI); WUS, WUSCHEL; ΔVirF, 51 amino acid translocation signal of VirF; LB/RB, left/right T-DNA border.

Strategy for visualization of simultaneous AMPT of two proteins into plant cells

The detection of the simultaneous translocation of two POIs and possibly also different combinations of POIs requires a versatile cloning platform. Although the 7x multimerized GFP_{11} tag significantly enhanced the sensitivity, we decided to continue with the single GFP_{11} or $Cherry_{11}$ tag as it resulted in sufficient fluorescence intensity and we suspected that a 7x tag might affect the functionality of the POI fused to it. We therefore replaced the $GFP_{11}:POI:\Delta virF$ coding region in the protein translocation plasmid by a synthetic fragment on which the individual

parts were separated by unique restriction sites, allowing easy exchange of plant promoter, POI coding region and vir promoter. As additional optimization, a leader (Shine and Dalgarno) sequence was placed before the ATG of the GFP₁₁ for improved translation and a linker sequence coding for 9 amino acids was placed between the GFP₁₁ tag and the region coding for the POI to minimize the chance that it would affect the functionality of the POI (Fig. 3A, Appendix 1a). This construct together with the previously plant optimized T-DNA construct carrying p35S::NLS:GFP₁₋₁₀::tNOS created the optimized split-GFP construct (split-GFP). For AMPT of a second protein, a synthetic fragment containing the same leader sequence upstream of a bacterium-optimized coding region for Cherry₁₁:POI:ΔvirF was cloned downstream of the $GFP_{11}:POI:\Delta virF$ coding region. Also here a linker sequence was added connecting the Cherry₁₁ and POI coding region (Appendix 1d). This generated a polycistronic operon where transcription from a *vir* gene promoter resulted in the production of a single RNA that is subsequently translated into two fusion proteins (Fig. 3B). For modulation of the ratio of expression of the two POI fusions, the positioning of the POI coding region inside the operon can be switched. The so-called transcription distance dictates that the open reading frame closer to the transcription start will be expressed at a higher level, because there is more time for translation (Lim et al., 2011). The presence of several unique restriction enzyme sites allows easy exchange of coding regions and vir promoters. We named this the double split fluorophore (ds-FP) system (Fig. 3B). The unique Xmal and BamHI restriction sites also allowed to add a second vir promoter depending on the experimental needs, thus creating two monocistronic operons, each with their own vir promoter (Fig. 3C). The p35S::NLS:Cherry₁₋₁₀::tNOS sequence was added to the T-DNA construct for detection of AMPT of Cherry₁₁fused proteins (Fig. 3D).

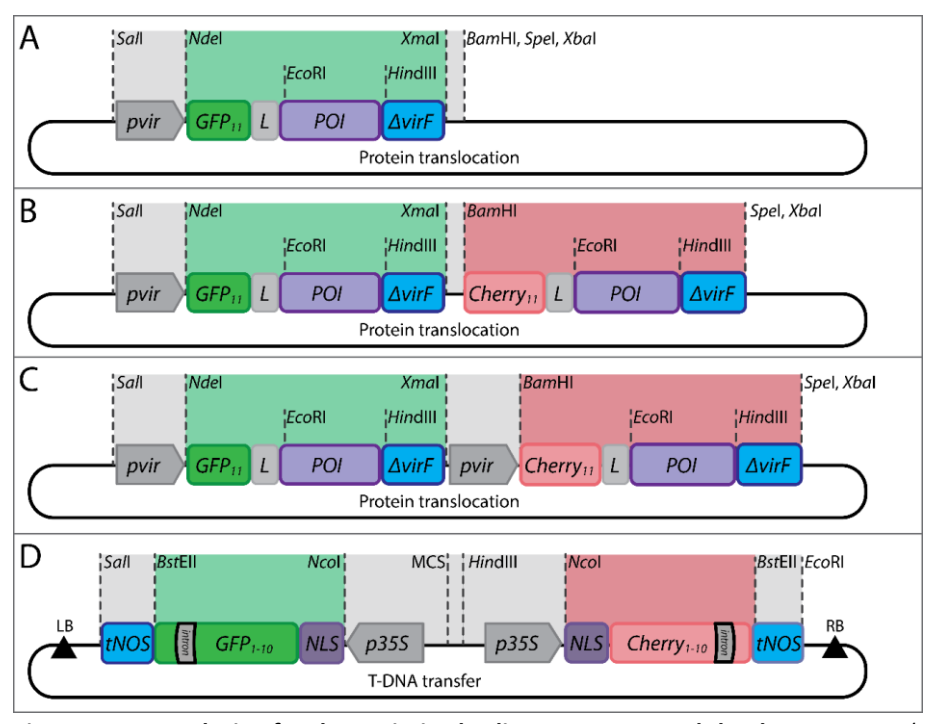


Figure 3. Vector design for the optimized split-GFP system and the ds-FP system. (A-D) All vectors were designed with unique restriction sites allowing easy exchange of individual components. (A) Protein translocation vector of the optimized split-GFP system with a coding region optimized for bacterial translation coding for GFP₁₁:POI:ΔVirF fusion protein expressed from a vir promoter (pvir). (B) Protein translocation vector for the ds-PF system with a vir promoter producing a polycistronic mRNA coding for the GFP₁₁:POI:ΔVirF and Cherry₁₁:POI:ΔVirF fusion proteins. (C) The protein translocation vector of the ds-FP system where the regions coding for the GFP₁₁:POI:ΔVirF and Cherry₁₁:POI:ΔVirF fusion proteins are transcribed from separate vir promoters. (D) T-DNA transfer vector used for both the split-GFP and ds-FP systems, containing a T-DNA carrying the p35S::NLS:GFP₁₋₁₀::tNOS and p35S::NLS:Cherry₁₋₁₀::tNOS genes to report AMPT of respectively GFP₁₁- or Cherry₁₁-tagged fusion proteins. The NLS:GFP₁₋₁₀ and NLS:Cherry₁₋₁₀ coding regions are codon-optimized for expression in plants and equipped with an intron to abolish expression in bacteria. Abbreviations: GFP, green fluorescent protein; tNOS, ΔVirF, 51 amino acid translocation signal of VirF; nopaline synthase transcriptional terminator; L, Linker sequence coding for 9 amino acids connecting the fluorophore 11 tag and the protein of interest (POI); p35S, Cauliflower Mosaic Virus 35S promoter; NLS, nuclear localization signal; LB/RB, left/right T-DNA border; MCS, multi cloning site.

Testing the ds-FP system for simultaneous AMPT of WUS and BBM to plant cells

As a first test of our newly designed ds-FP system, we infiltrated 4-weeks old tobacco leaves with an Agrobacterium strain containing the protein translocation vector pvirF::GFP₁₁:WUS:ΔvirF with bacterial codon optimized WUS (Appendix 1f) and the T-DNA construct p35S::NLS:GFP₁₋₁₀::tNOS/p35S::NLS:Cherry₁₋₁₀::tNOS to report AMPT of the GFP₁₁-tagged fusion protein (Fig. 4A). Clear nuclear GFP fluorescence was detected at 4 dpi (Fig. 4B), indicating that the split-GFP reporter of the new ds-FP system successfully detected AMPT. Next, we tested both split-GFP and split-Cherry reporters in combination with the polycistronic vector for expression in Agrobacterium. Tobacco leaves were infiltrated with an Agrobacterium strain containing the polycistronic pvirF::GFP₁₁:WUS:ΔvirF-Cherry₁₁:BBM:ΔvirF protein translocation vector and the p35S::NLS:GFP₁₋ 10::tNOS/p35S::NLS:Cherry1-10::tNOS T-DNA AMPT reporter construct (Fig. 4C). At 4 dpi again clear nuclear GFP fluorescence was detected, however, no Cherry fluorescence was observed (Fig. 4D). Introduction of the virD promoter in front of the *Cherry*₁₁:*BBM*:∆*virF* coding region also did not result in detectable Cherry fluorescence, whereas AMPT of the GFP₁₁:WUS:ΔVirF fusion protein still resulted in nuclear GFP signal (Fig. S1A, S1B). To rule out design problems with the ds-FP system, a single split-Cherry system was constructed by replacing *pvirF::GFP*₁₁:WUS:ΔvirF in the protein translocation vector by pvirF::Cherry₁₁:WUS:ΔvirF and replacing p35S::NLS:GFP₁₋₁₀::tNOS in the T-DNA transfer vector by p35S::NLS:Cherry₁₋₁₀::tNOS (Fig. S1C). Infiltrating tobacco leaves with an Agrobacterium strain carrying the resulting single split-Cherry system did not result in detectable Cherry fluorescence at 4 dpi (Fig. S1D). The very bright Cherry fluorescence obtained when both split-Cherry components, Cherry₁₁:WUS:ΔvirF and NLS:Cherry₁₋₁₀, are expressed from the 35S promoter (Figure 2A, B) suggests that the Cherry₁₁ tag somehow prevents translocation of the fusion protein to the plant cell. Interestingly, the GFP fluorescence observed from the ds-FP system was significantly (1.4-fold) higher compared to the split-GFP system (Fig 4E). Somehow *GFP*₁₁: WUS: ΔvirF expression from the polycistronic operon is more efficient than from the monocistronic operon.

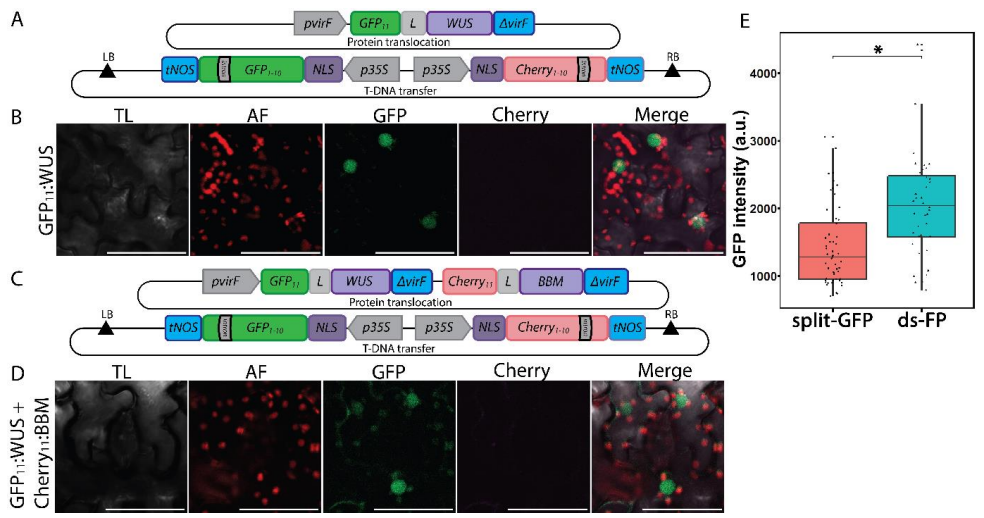


Figure 4. The ds-FP system detects AMPT of GFP₁₁-tagged but not of Cherry₁₁-tagged proteins. (A, C) The ds-FP system with the protein translocation construct coding for the GFP₁₁:WUS:ΔVirF fusion (split-GFP, A) or for both the GFP₁₁:WUS:ΔVirF and the Cherry₁₁:BBM:GFP₁₁:WUS:ΔVirF fusion (ds-FP, C). Both T-DNA transfer constructs express NLS:GFP₁₋₁₀ and NLS:Cherry₁₋₁₀ from the *35S* promoter. See also Figure 3 for further information. (B, D) Confocal microscopy images of leaf epidermis cells of 4-weeks old tobacco plants at 4 dpi with an Agrobacterium strain carrying the split-GFP system depicted in (A) or the ds-FP system depicted in (C). Scale bars indicate 50 μm. Abbreviations: TL, transmitted light; AF, autofluorescence; WUS, WUSCHEL; BBM, BABY BOOM. (E) Quantification of the intensity of the nuclear GFP signal in tobacco mesophyll cells after AMPT using the split-GFP (B) or the ds-FP (D) system. For each treatment 50 nuclei were measured in 18 images taken from the 3th, 4th and 5th leaf of six tobacco plants. The dots indicate the fluorescence intensity per nucleus. The statistically significant difference is indicated above boxplots (*: p < 0.05) as determined by the Student's *t*-test with Tukey's honest significant difference post hoc test.

Use of split GFP and Cherry for detection of simultaneous AMPT and AMT to plant cells

Although the split Cherry system appeared unsuitable as reporter for AMPT, our results did show that the Cherry reporter is a good marker to detect T-DNA transfer (Fig. 2B). We therefore decided to use it in combination with the split GFP reporter for the simultaneous detection of respectively AMT and AMPT (referred to as the

split-GFP^{col} system), allowing to compare the efficiencies of the two processes, not only in tobacco, but also in plant species or genotypes that are more recalcitrant to transformation. The transient Cherry expression following T-DNA transfer can also be used as a positive control for successful leaf infiltration and activation of the Agrobacterium *vir* system by the host cells. This is important, as many economically important crop plants commonly used in various laboratory experiments show recalcitrance to AMT. In laboratory experiments, the tomato cultivar 'Moneymaker' is popular but shows low leaf transformation efficiency (Hoshikawa et al., 2019) and subsequent regeneration proves laborious (Eck et al., 2019). Plant defense responses against Agrobacterium were reported to contribute significantly to limit or completely inhibit AMT (Pitzschke, 2013).

For the simultaneous detection of AMT and AMPT, the T-DNA transfer vector was equipped with the optimized NLS:GFP₁₋₁₀ and NLS:Cherry coding regions, both expressed under control of the 35S promoter (Fig. 5A) and the protein translocation vector carrying pvirF::GFP₁₁:WUS:ΔvirF was used (Fig. 5A). An Agrobacterium strain containing this split-GFP^{col} system was used to infiltrate leaves of 4 weeks old plants of tobacco and of the crop species tomato (Solanum lycopersicum cv. 'Money Maker'), pepper (Capsicum annuum cv. 'jalapeño') and rapeseed (Brassica napus subsp. oleifera). As observed previously (Fig. 2B and 2D), tobacco leaf epidermis cells showed a strong Cherry signal, marking cells transformed with the T-DNA construct. As previously observed, the GFP signal observed in the nucleus of the same cells was weaker and even absent in some cells that were marked by a clear Cherry signal. Assuming that T-DNA transfer always coincides with protein translocation, this indicates that AMPT occasionally is not detected because the number of translocated fusion proteins is too low, and that despite the improved split-GFP system this results in an underestimation of the frequency of AMPT. In tomato leaves also clear signals were observed for both AMT and AMPT, however in leaves of sweet pepper and rapeseed the Cherry and GFP signals were significantly weaker (Fig. 5B). These results show that the split-GFP^{col} system can be used in varieties of common crop plant species to report simultaneous AMPT and AMT, and thus may provide an useful tool to analyze and resolve bottle necks in transformation and regeneration.

The model plant *Arabidopsis thaliana* is also considered recalcitrant for transient transformation assays, limiting its use for rapid studies of *in planta* protein localization and interaction. Leaf infiltration protocols for *Arabidopsis* have been optimized to include prolonged induction of Agrobacterium with acetosyringone (Mangano et al., 1998), different Agrobacterium strains (Wroblewski et al., 2005) or infiltrating higher bacterial concentrations into leaves (Y. Zhang et al., 2020). However, the use of Arabidopsis cell suspension cultures has until now been limited to protoplast isolation and subsequent chemical transformation. Here we tested the split-GFP^{col} system on Arabidopsis cell suspensions and to our surprise we detected clear nuclear split-GFP signals, indicative of AMPT, co-localizing with nuclear Cherry signals indicative of AMT (Fig. S2). These results show that the split-GFP^{col} system can be used for the detection of AMPT and AMT in both leaves of different plant species (tobacco, tomato, pepper and rapeseed) and in Arabidopsis suspension cells.

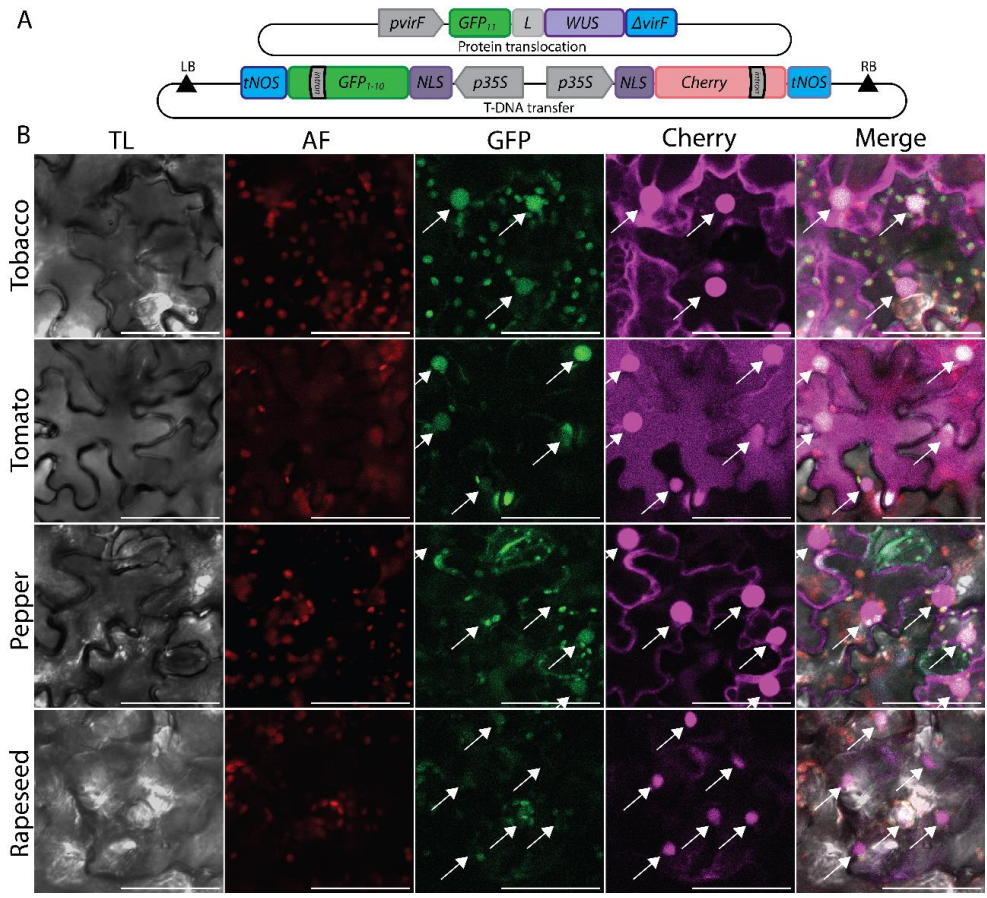


Figure 5. The use of split-GFP and Cherry (split-GFP^{col}) to detect simultaneous AMPT and AMT, respectively. (A) Schematic representation of the combined AMPT/AMT detection system split-GFP^{col}. The system comprises a T-DNA transfer vector containing the optimized *NLS:GFP*₁₋₁₀ and *NLS:Cherry* coding regions, both expressed from the *35S* promoter. The protein transfer vector encodes a GFP₁₁-WUS- Δ VirF fusion protein expressed from the *virF* promoter. See Figure 3 for further information. (B) Confocal microscopy images of leaf epidermis cells of 4-weeks old plants of the indicated plant species. Arrows indicate colocalized GFP and Cherry fluorescence in the nucleus, indicative of simultaneous AMPT and AMT. Scale bars indicate 50 μ m. Abbreviations: TL, transmitted light; AF, autofluorescence.

Discussion

In this study, the split-GFP system previously developed to visualize AMPT in plants was optimized for better translational efficiency of the individual components in

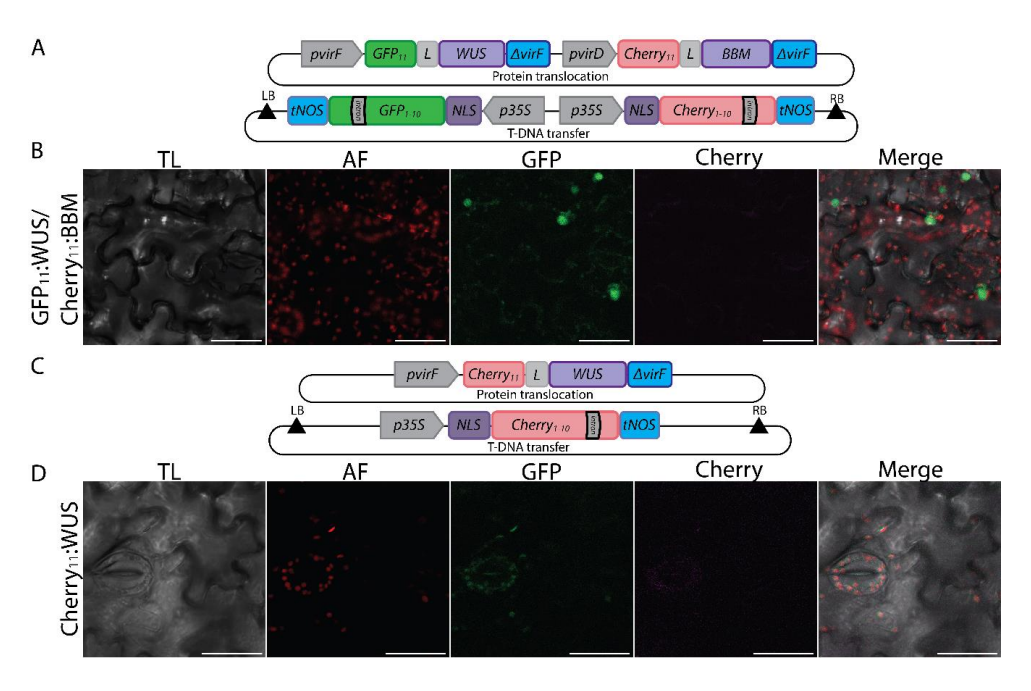
either Agrobacterium (GFP₁₁ fusion protein) or plant cells (GFP₁₋₁₀). This resulted in significantly higher GFP fluorescence intensity and thus increased the sensitivity of AMPT detection, allowing to reduce the laser power of the confocal microscope, thus preventing photobleaching and phototoxicity (Colin et al., 2022). A further increase in the GFP intensity was achieved by multimerization of the GFP₁₁ tag (GFP₁₁x7). As indicated, however, we decided not to use this, as we suspected that a repeated GFP₁₁ tag might interfere with the functionality of the POI fused to it, especially when it leads to reconstitution of multiple GFPs.

To visualize AMPT of two POIs either tagged with either GFP₁₁ or Cherry₁₁, an additional split fluorophore system (split-Cherry) was added to this optimized split-GFP system. In order to express two fluorophore-tagged proteins from a single plasmid, we either placed both coding regions in a single operon expressed from the same vir promoter or in two separate operons, each expressed from its own vir promoter. The single operon construct gave sufficient expression to detect AMPT of GFP₁₁-tagged WUS and interestingly the fluorescence was significantly higher than when the GFP₁₁-tagged WUS proteins was expressed from a monocistronic operon. This confirmed the observations in *E. coli* where increasing the operon length resulted in increased expression (Lim et al., 2011). Nonetheless, we were not able to detect AMPT of the Cherry₁₁-BBM fusion, also not when expressed from its own vir promoter. This despite the fact that our results clearly showed that the split-Cherry system works in plants when both parts are expressed from the same plasmid. The most likely reason for this is that the Cherry₁₁ tag prevents AMPT of the fusion protein. Possibly, the linker length or spatial arrangement of the fusion protein is limiting the transfer through the T4SS pilus. A second reason might be that the sensitivity of the split-Cherry system is insufficient to detect AMPT. Based on the experiments presented in this chapter, we cannot exclude any of these options.

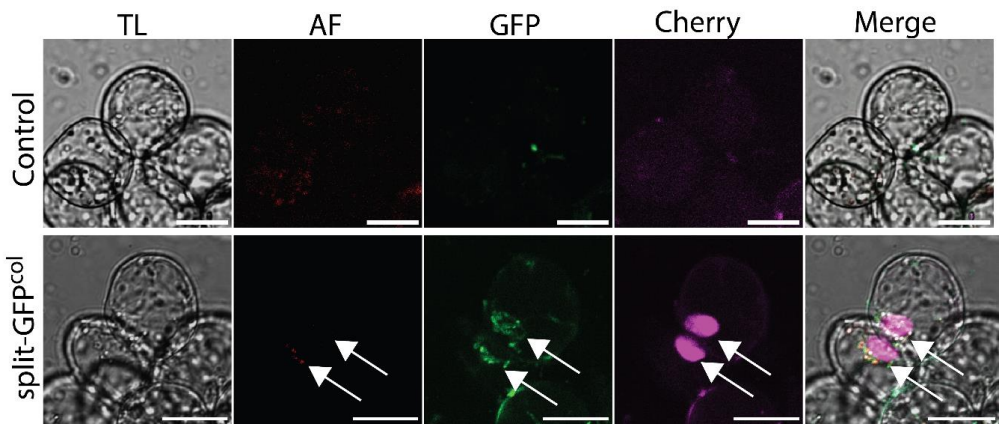
The Cherry fluorophore appeared to be a useful reporter to detect transient expression following AMT. As such, it was used in the split-GFP^{col} system to detect simultaneous AMT and AMPT in different plant species. The potential use of the split-GFP system to detect AMPT has previously been demonstrated in various plant species, such as *N. tabacum*, *N. benthamiana*, *Arabidopsis* and tulip (Khan,

2017). Here we confirmed this for tobacco, but also showed that it is possible to detect AMT and AMPT in tomato, pepper, rapeseed and for the first time in Arabidopsis suspension cells. The *Arabidopsis* cell suspension system provides a readily available and continuous supply of close to identical cells, enabling more high-throughput visualization of a variety of fusion proteins and a foundation for upscaling for fusion protein extraction or transient produced compound extraction. Both in previous work as well as in the experiments performed in this chapter, the overexpression of full length GFP or Cherry led to fluorescence observed both in the nucleus as in the cytosol. NLS activity can vary depending on flanking sequences and the target organism (Kosugi et al., 2009). The NLS sequence might be optimized to prevent signal dispersion, but in our case the cytosolic signal was also indicative for the efficiency of AMT, which was higher for tobacco and tomato and lower for pepper and rapeseed, plant species known to be more recalcitrant to AMT. As expected, the GFP fluorescence intensity marking AMPT correlated with the Cherry fluorescence intensity.

Supplementary figures



Supplementary figure 1. The split-Cherry system is not suitable for detecting AMPT. (A) Schematic representation of the ds-FP system where the regions coding for the GFP₁₁:WUS:ΔVirF and Cherry₁₁:BBM:ΔVirF fusion proteins are transcribed from respectively the *virF* or *virD* promoter from the protein translocation vector. The T-DNA transfer vector carries *p35S::NLS:GFP₁₋₁₀::tNOS* and *p35S::NLS:Cherry₁₋₁₀::tNOS* to report AMPT of both the GFP₁₁- and Cherry₁₁-tagged fusion proteins (B) Confocal microscopy images of leaf epidermis cells of 4-weeks old tobacco plants at 4 dpi with an Agrobacterium strain carrying the ds-FP system depicted in (A). (C) Schematic representation of the optimized split-Cherry system with a protein translocation vector coding for the Cherry₁₁:WUS:ΔVirF fusion protein expressed from the *virF* promoter and the T-DNA transfer vector carrying *p35S::NLS:Cherry₁₋₁₀::tNOS* to report AMPT of the Cherry₁₁-tagged fusion protein. (D) Confocal microscopy images of leaf epidermis cells of 4-weeks old tobacco plants at 4 dpi with an Agrobacterium strain carrying the split-Cherry system depicted in (C). Scale bars indicate 50 μm. Abbreviations: TL, transmitted light; AF, autofluorescence.



Supplementary figure 2. The use of split-GFP and Cherry (split-GFP^{col}) to detect simultaneous AMPT and AMT in Arabidopsis suspension cells. Confocal microscopy images of Arabidopsis suspension cells after 4 days of cocultivation with an Agrobacterium strain carrying a control vector (p35S::NLS:GFP₁₋₁₀::tNOS/p35S::NLS:Cherry₁₋₁₀::tNOS) or the split-GFP^{col} system (p35S::NLS:GFP₁₋₁₀::tNOS/p35S::NLS:Cherry::tNOS + pvirF::GFP₁₁:WUS:ΔvirF). Scale bars indicate 50 μm. White arrows indicate the position of GFP and Cherry positive nuclei. Abbreviations: TL, transmitted light; AF, autofluorescence.

Appendix

Appendix 1. (a-f) DNA sequences coding for: (a) empty bacterial codon optimized split-GFP construct, (b) plant codon optimized sfGFP₁₋₁₁, (c) plant codon optimized sfCherry2₁₋₁₁, (d) empty bacterial codon optimized ds-FP cloning construct (*pvir::leader*

sequence:sfGFP₁₁:linker:POI:ΔvirF:pvir::leader sequence:sfCherry2₁₁:linker:POI:ΔvirF), (e) bacterial codon optimized BBM and (f) bacterial codon optimized WUS. Highlighted are: the NLS sequence in purple, the intron sequence in yellow, the sfCherry2₁₁ part in red, the sfGFP₁₁ part in green and the linker sequence in grey. Promoter, POI, Leader (Shine & Dalgarno) sequence. start and stop sequences are in bold. Restriction enzyme recognition sites are underscored.

ATGGAGCTTTGAAGGGAGAAATTAATCAAAGATTGAAGTTGAAGGATGGAGGACATTATGA
TGCTGAAGTTAAGACTACTTATAAGGCTAAGAAGCCTGTTCAATTGCCTGGAGCTTATAATGT
TGATATTAAGTTGGATATTACTTCTCATAATGAAGATTATACTATTGTTGAACAATATGAAAG
AGCTGAAGCTAGACATTCTACTTAA

- e) GAATTCAACAACAACTGGCTGGGCTTCTCCCTGTCCCCGTACGAACAGAACCACCACCGCAA GGACGTCTGCTCCACCACCACCACCGCCGTTGACGTCGCCGGCGAATACTGCTACGACCC GACCGCCGCCTCCGACGAATCCTCCGCCATCCAGACCTCCTTCCCGTCCCCGTTCGGCGTCGT CCTGGACGCCTTCACCCGCGACAACACTCCCACTCCCGCGACTGGGACATCAACGGCTCCG CCTGCAACACCACCACGACGACGACGACGCCCGAAGCTGGAAAACTTCCTGGGCCG CACCACCACCATCTACAACACCAACGAAAACGTCGGCGACATCGACGGCTCCGGCTGCTACG GCGGCGGCGCGGCGGCGGCTCCCTGGGCCTGTCCATGATCAAGACCTGGCTGCGCAA CCAGCCGGTTGACAACGTTGACAACCAGGAAAACGGCAACGGCCCAAGGGCCTGTCCCTG TCCATGAACTCCTCCACCTCCTGCGACAACAACAACTACTCCTCCAACAACCTGGTCGCCCAG GGCAAGACCATCGACGACTCCGTCGAAGCCACCCCGAAGAAGACCATCGAATCCTTCGGCCA GCGCACCTCCATCTACCGCGGCGTCACCCGCCACCGCTGGACCGGCCGCTACGAAGCCCACC TGTGGGACAACTCCTGCAAGCGCGAAGGCCAGACCCGCAAGGGCCGCCAGGTCTACCTGGG CGGCTACGACAAGGAAGAAAAGGCCGCCCGCGCCTACGACCTGGCCGCCCTGAAGTACTGG GGCACCACCACCACCACCACCTCCCGATGTCCGAATACGAAAAGGAAATCGAAGAAATGAA GCACATGACCCGCCAGGAATACGTCGCCTCCCTGCGCCAAGTCCTCCGGCTTCTCCCGCG GCGCCTCCATCTACCGCGGCGTCACCCGCCACCACCAGCACGGCCGCTGGCAGGCCCGCATC GGCCGCGTCGCCGGCAACAAGGACCTGTACCTGGGCACCTTCGGCACCCAGGAAGAAGCCG CCGAAGCCTACGACATCGCCGCCATCAAGTTCCGCGGCCTGACCGCCGTCACCAACTTCGAC ATGAACCGCTACAACGTCAAGGCCATCCTGGAATCCCCGTCCCTGCCGATCGGCTCCGCCGCC AAGCGCCTGAAGGAAGCCAACCGCCCGGTCCCGTCCATGATGATCTCCAACAACGTCTC CGAATCCGAAAACAACGCCTCCGGCTGGCAGAACGCCGCCGTCCAGCACCACCAGGGCGTT GACCTGTCCCTGCTGCAGCAGCACCAGGAACGCTACAACGGCTACTACTACAACGGCGGCAA CCTGTCCTCCGAATCCGCCCGCGCCTGCTTCAAGCAGGAAGACGACCAGCACCACTTCCTGTC CAACACCCAGTCCCTGATGACCAACATCGACCACCAGTCCTCCGTCTCCGACGACTCCGTCAC CGTCTGCGGCAACGTCGTCGGCTACGGCGGCTACCAGGGCTTCGCCGCCCCGGTCAACTGCG ACGCCTACGCCGCCTCCGAGTTCGACTACAACGCCCGCAACCACTACTACTTCGCCCAGCAGC

AGCAGACCCAGCACTCCCCAGGCGGCGACTTCCCGGCCGCCATGACCAACAACGTCGGCTCC AACATGTACTACCACGGCGAAGGCGGCGCGAAGTCGCCCCGACCTTCACCGTCTGGAACG ACAACAAGCTT

Materials and methods

Agrobacterium strains and growth conditions

The Agrobacterium strain AGL1 (C58, *RecA*, pTiBo542 disarmed, Rif, Cb) (Jin et al., 1987) used in this chapter was grown in modified LC medium (10 g/L tryptone, 5 g/L yeast extract, 5 g/L NaCl, pH = 7.5) at 28 °C with the appropriate antibiotics at the following concentrations: gentamicin 40 μ g/ml; carbenicillin 75 μ g/ml; kanamycin 100 μ g/ml; rifampicin 20 μ g/ml. Plasmids were introduced into Agrobacterium by electroporation, as previously described (den Dulk-Ras & Hooykaas, 1995).

Plant growth conditions

The seeds of *Nicotiana tabacum* cv. Petit Havana SR1, *Nicotiana benthamiana, Capsicum annuum cv. 'Jalapeño'* (hot pepper) and *Solanum lycopersicum* cv.

'Money Maker' (tomato) were stratified for seven days on wet soil and germinated

in high humidity under a plastic cover and seedlings were grown in growth chambers at 24 °C, 75 % relative humidity and a 16 hours photoperiod for four weeks.

The seeds of *Brassica napus* (rapeseed) were germinated in high humidity under a plastic cover and seedlings were grown in growth chambers at 21 °C, 50 % relative humidity and a 16 hours photoperiod for four weeks.

The Arabidopsis thaliana T87 cell suspension was derived from seedlings of Arabidopsis thaliana (L.) Heynh. Accession Columbia (Axelos et al., 1992). The cell suspension was maintained as previously described (Ostergaard et al., 1996) under continuous light at 22°C with rotary shaking at 120 rpm and subcultured at 7-day intervals. The cell culture medium consisted of a modified B5 medium (Gamborg et al., 1968) with 30 g/L sucrose and 1 μ M NAA.

Agrobacterium leaf infiltration and cell suspension co-cultivation

For co-cultivation, a colony of Agrobacterium strain AGL1 with the appropriate plasmids (overview plasmids: Table 1) from a fresh one-week old plate was resuspended in 10 ml LC medium (10 g/L tryptone, 5 g/L yeast extract, 5 g/L NaCl, pH = 7.5) supplemented with the appropriate antibiotics in a 100 ml Erlenmeyer flask and was incubated at 28 °C under continuous shaking (180 rpm) until the culture reached an OD $_{600}$ of 1.0. The bacteria were pelleted by centrifugation in a 50 ml tube (CLS430829, Corning) at 4000 rpm for 20 minutes and resuspended in 20 ml AB minimal medium (Gelvin, 2006) with the appropriate antibiotics and grown overnight at 28 °C under continuous shaking (180 rpm) until an OD $_{600}$ of 0.8. The bacteria were pelleted as described above and resuspended in 20 ml induction medium (Gelvin, 2006) containing 200 μ M acetosyringone. The bacteria were induced overnight in induction medium in the dark on a rocking shaker at 60 rpm at room temperature. Prior to infiltration, the overnight cultures were pelleted as described above and resuspended in half-strength MS medium (Murashige & Skoog, 1962) to an OD $_{600}$ of 0.8.

For the detection of AMPT or AMT, the 3th, 4th and 5th leaves of four weeks old plants were infiltrated on the abaxial side using a blunt tipped 5 ml syringe with an induced Agrobacterium culture. After infiltration the plants were covered with

plastic overnight, after which the plastic was removed and the plants were incubated for three more days. Leaf discs obtained from the infiltrated parts of the leaf were placed on a microscopy slide in water, covered with a cover slip and the abaxial side of the leaf observed under the confocal microscope at 4 days post infiltration.

For cell suspension co-cultivation, five days after subculture 1.5 ml of *Arabidopsis* cell suspension was transferred to a 6-wells plate and 1.5 ml of induced Agrobacterium culture was added to a final concentration of $OD_{600} = 0.4$. After 36 hours under normal growth conditions the co-cultivation medium was replaced by fresh cell culture medium with 250 µg/L Timentin. The suspension cells were visualized using confocal microscopy at four days after co-cultivation.

Laser scanning confocal microscopy

Fluorescence was observed using a Zeiss Imager M1 or a Zeiss observer (Zeiss, Oberkochen, Germany) confocal laser scanning microscope, equipped with an LSM 5 Exciter using a 20x and 40x magnifying objective (numerical aperture of 0.8 and 0.65, respectively). GFP signal was detected using an argon 488 nm laser and a 505-530 nm band-pass emission filter. Chloroplast- and other auto-fluorescence was detected using an argon 488 nm laser and a 650 nm long pass emission filter. Cherry signal was detected using a 561 nm Diode laser and a 595 – 500 nm band-pass filter. Visible light was detected using the transmitted light detector. Images were collected using ZEN black edition (Zeiss, Oberkochen, Germany) imaging software and processed in ImageJ (Schneider et al., 2012). The GFP or Cherry fluorescence intensity was measured in ImageJ.

Plasmid construction

The plasmids described in this chapter are listed in Table 1. All cloning steps were performed in *E. coli* strain DH5 α (CGSC#: 14231) (Laboratories, 1986). PCR amplifications were done with Phusion High-Fidelity DNA Polymerase (Thermo Scientific, Landsmeer, the Netherlands) and resulting plasmids were verified by

sequencing. Primers used to construct the plasmids are listed in Table 2. Sequences were codon optimized using the web base tool OPTIMIZER (Puigbò et al., 2007).

For the T-DNA transfer construct, a modified version of the plasmid pSDM3764 (Khan, 2017), originating from pCambia1302, a derivative of the pPZP family of binary plasmids (Hajdukiewicz et al., 1994), was used. The pSDM3764 plasmid harbours a GFP₁₋₁₀ sequence under control of the Cauliflower Mosaic Virus 35S promoter (p35S) and the terminator of the nopaline synthase gene (tNOS) (Sakalis et al. 2013). To engineer the optimized split-GFP construct, the NLS:GFP₁₋₁₀ sequence of the T-DNA plasmid, pSDM3764, was replaced by restriction enzyme digestion with Ncol and BstEII with a plant codon optimized NLS:GFP₁₋₁₀opt synthetic sequence (Bio Basic inc., Canada) containing an 84 nucleotide intron IV sequence of the potato ST-LS1 gene (Pang et al., 1996) (Appendix 1b). To engineer the doublesplit fluorophore (ds-FP) system, the optimized split-GFP plasmid was digested with BamHI and EcoRI and a synthetic sequence coding for NLS:sfCherry2₁₋₁₀opt (Appendix. 1c) driven by p35S and terminated by tNOS was inserted. To construct the AMT and AMPT co-localization construct instead of NLS:sfCherry2₁₋₁₀opt a synthetic sequence coding for NLS:sfCherry2opt was inserted into the ds-FP T-DNA transfer construct using the BamHI and EcoRI restriction sites.

The protein translocation vector was based on pSDM6503 (Khan, 2017), a modified version of the plasmid pSDM3163 (Sakalis et al., 2014a). Plasmid pSDM6503 harbours a coding region consisting of an AHL15 sequence N-terminally tagged via a 27 bp linker sequence to GFP_{11} and C-terminally to $\Delta virF$, under control of the virF promoter (Khan, 2017). To engineer the optimized split-GFP construct (split-GFP°), the open reading frame and adjacent multicloning site were removed by digesting the vector with NdeI and XbaI, and inserting a compatible synthetic DNA fragment coding for bacterial codon optimized GFP_{11}^{opt} : $Linker:\Delta virF$ (Appendix 1a) and with a leader sequence (L) containing a Shine-Dalgarno sequence (AGGAGC) preceding the translation initiation start site (ATG) at a previously determined optimal seven base pairs distance (Shultzaberger et al., 2001) (Fig 3A). The resulting construct (split-GFP°) was used to insert any gene of interest, bacterial codon optimized, using the restriction enzymes EcoRI and HindIII. To construct the double-split fluorophore system (ds-FP), the split-GFP°pt vector was digested with XmaI and SpeI. A synthetic

DNA sequence was inserted coding for bacterial codon optimized $sfCherry2_{11}^{opt}:Linker:\Delta virF$. The fragment contains a leader sequence on which a Shine-Dalgarno sequence (Shine & Dalgarno, 1974) had been placed, thereby creating a polycistronic construct driven by one promoter (Fig. 3B, Appendix 1d). To create a ds-FP with each fluorophore driven by a separate promoter, the construct was digested with the restriction enzymes Xmal and BamHI to insert a PCR fragment with Xmal and BamHI restriction sites containing the virD promoter in front of the $sfCherry2_{11}^{opt}:LinkerPGOI:\Delta virF$ sequence (Fig. 3C).

Table 1. Plasmids and their combinations used in this study. Km^r = Kanamycin A Gm^r = Gentamycin. In the main text sfCherry2 is referred to as Cherry and the optimized superscript (opt) is omitted.

Plasmid content	Function	Source
p35S::NLS:GFP ₁₋₁₀ ::tNOS/pNOS::Hyg	T-DNA transfer (Km ^r)	Khan, 2017
p35S::NLS:GFP ₁₋₁₀ °pt::tNOS / pNOS::Hyg	T-DNA transfer (Km ^r)	Chapter 2
p35S::NLS:sfCherry ₁₋₁₀ opt::tNOS / pNOS::Hyg	T-DNA transfer (Km ^r)	Chapter 2
p35S::NLS:GFP ₁₋₁₀ ^{opt} ::tNOS/ p35S::NLS:sfCherry ₁₋₁₀ ^{opt} ::tNOS/pNOS::Hyg	T-DNA transfer (Km ^r)	Chapter 2
p35S::NLS:GFP ₁₋₁₀ °pt::tNOS/p35S::NLS:sfCherry-°pt::tNOS/pNOS::Hyg	T-DNA transfer (Km ^r)	Chapter 2
pvirF::GFP ₁₁ :BBM:ΔvirF	Protein translocation (Gm ^r)	Khan, 2017
pvirF::GFP ₁₁ ^{opt} :BBM ^{opt} :ΔvirF	Protein translocation (Gm ^r)	Chapter 2
pvirF::GFP ₁₁ ^{opt} :WUS ^{opt} :ΔvirF	Protein translocation (Gm ^r)	Chapter 2
pvirF::GFP ₁₁ ^{opt} :WUS ^{opt} :ΔvirF:sfCherry2 ₁₁ ^{opt} :BBM ^o ^{pt} :ΔvirF	Protein translocation (Gm ^r)	Chapter 2
$pvirF::GFP_{11}^{opt}:WUS^{opt}:\Delta virF:pVirD::sfCherry2_{11}^{op}$ $^{t}:BBM^{opt}:\Delta virF$	Protein translocation (Gm ^r)	Chapter 2
pvirF::sfCherry2 ₁₁ ^{opt} :WUS ^{opt} :ΔvirF	Protein translocation (Gm ^r)	Chapter 2
pvirF::GFP ₁₁ x7 ^{opt} :BBM ^{opt} :ΔvirF	Protein translocation (Gm ^r)	Chapter 2

Table 2. Overview of primers used in this study

Primer name	Sequence
BamHI- ΔVirF -OPT Fw	<u>GGATCC</u> TCATAGACCGCGCGTTGA
Ndel-GFP11-OPT Rev	<u>CATATG</u> CGCGACCACATGGTCCTG
Sall pVirD Fw	<u>GTCGAC</u> AAACGGAGTGCATTTGTATTTTTG
Sall pVirF Fw	<u>GTCGAC</u> CCTATGATAGTCGATATTTTGGTCCG
Sall pVirE Fw	<u>GTCGAC</u> CGGCTGCTCGTCACCAACAA
Ndel pVirD Rev	<u>CATATG</u> CTTCCTCCAAAAAAAGCGGAAG
Ndel pVirE Rev	<u>CATATG</u> TTCTCTCCTGCAAAATTGCGGTTT
Ndel-pVirF Rev	<u>CATATG</u> ATCGCTCCTGTGCTTTTGAAAG
GFP11x7 Fw opt	CATATGCGCGACCACATGGTC
GFP11x7 Rev opt	GAATTC GGAGCCGCCCC
HindIII 35S Cherry	CCC <u>AAGCTT</u> CATGGAGTCAAAGATTCAAAT
EcoRI NOS Cherry	CCG <u>GAATTC</u> CCCGATCTAGTAACATAGATGAC
Ndel SfCherry11	G <u>GAATTCCATATG</u> ATGTACACCATCGTCGAACAG
EcoRI SfCherry11	G <u>GAATTC</u> GGAGCCGCCGC
pSDM6500 Seq Fw	GTGATCATTTGCAGTATTCG
pSDM6500 Seq Rev	CAAGGCGATTAAGTTGGGTAA
pCambia1300 Seq Fw	CGTATGTTGTGGAATTGTGAGC
pCambia1300 Seq Rev	CACGGGGACTCTTGACCATG

Acknowledgements

The authors would like to thank Gerda Lamers and Joost Willemse for their assistance with the microscopy experiments, Ward de Winter and Jan Vink with their help supplying media, cell suspension cultures and caretaking of the growth

rooms. We would like the thank Tim Harmsen for his assistance and collaborating in optimizing the cell suspension transformation protocol. We acknowledge Richard den Os for his help in constructing plasmids and optimizing the plate reader experiments.

Author contribution

Ivo Gariboldi, Maarten Stuiver and Remko Offringa conceived and designed the experiments. Ivo Gariboldi, Jaap Tromp, Koen van Oostrom and Anton Rotteveel constructed plasmids, performed the experiments and performed the microscopic analysis. Ivo Gariboldi and Jaap Tromp performed statistical analysis. Ivo Gariboldi and Remko Offringa analyzed the results and wrote the manuscript.

References

- Axelos, M., Curie, C., Mazzolini, L., Bardet, C., & Lescure, B. (1992). A protocol for transient gene expression in Arabidopsis thaliana protoplasts isolated from cell suspension cultures. *Plant Physiology and Biochemistry*, *30*, 123–128. https://api.semanticscholar.org/CorpusID:80736222
- Colin, L., Martin-Arevalillo, R., Bovio, S., Bauer, A., Vernoux, T., Caillaud, M. C., Landrein, B., & Jaillais, Y. (2022). Imaging the living plant cell: From probes to quantification. *Plant Cell*, 34(1), 247–272. https://doi.org/10.1093/plcell/koab237
- den Dulk-Ras, A., & Hooykaas, P. J. J. (1995). Electroporation of Agrobacterium tumefaciens. In J. A. Nickoloff (Ed.), *Plant Cell Electroporation and Electrofusion Protocols* (pp. 63–72). Springer New York. https://doi.org/10.1385/0-89603-328-7:63
- Eck, J. Van, Keen, P., & Tjahjadi, M. (2019). Agrobacterium tumefaciens-Mediated Transformation of Tomato. *Transgenic Plants. Methods in Molecular Biology, 1864*, 225–234. ttps://doi.org/10.1007/978-1-4939-8778-8_16
- Feng, S., Sekine, S., Pessino, V., Li, H., Leonetti, M. D., & Huang, B. (2017). Improved split fluorescent proteins for endogenous protein labeling. *Nature Communications*, 8(1). https://doi.org/10.1038/s41467-017-00494-8
- Gamborg, O. L., Miller, R. A., & Ojima, K. (1968). Nutrient requirements of suspension cultures of soybean root cells. *Experimental Cell Research*, *50*(1), 151–158. https://doi.org/10.1016/0014-4827(68)90403-5
- Gelvin, S. B. (2006). Agrobacterium virulence gene induction. *Methods in Molecular Biology* (*Clifton, N.J.*), 343, 77–84. https://doi.org/10.1385/1-59745-130-4:77

- Ghosh, I., Hamilton, A. D., & Regan, L. (2000). Antiparallel leucine zipper-directed protein reassembly: Application to the green fluorescent protein [12]. *Journal of the American Chemical Society*, 122(23), 5658–5659. https://doi.org/10.1021/ja994421w
- Hajdukiewicz, P., Svab, Z., & Maliga, P. (1994). The small, versatile pPZP family of Agrobacterium binary vectors for plant transformation. *Plant Molecular Biology*, 25(6), 989–994. https://doi.org/10.1007/BF00014672
- Haseloff, J., Siemering, K. R., Prasher, D. C., & Hodge, S. (1997). Removal of a cryptic intron and subcellular localization of green fluorescent protein are required to mark transgenic Arabidopsis plants brightly. *Proceedings of the National Academy of Sciences*, 94(6), 2122–2127. https://doi.org/10.1073/pnas.94.6.2122
- Hoshikawa, K., Fujita, S., Renhu, N., Ezura, K., Yamamoto, T., Nonaka, S., Ezura, H., & Miura, K. (2019). Efficient transient protein expression in tomato cultivars and wild species using agroinfiltration-mediated high expression system. *Plant Cell Reports*, 38(1), 75–84. https://doi.org/10.1007/s00299-018-2350-1
- Kamiyama, D., Sekine, S., Barsi-Rhyne, B., Hu, J., Chen, B., Gilbert, L. A., Ishikawa, H., Leonetti, M. D., Marshall, W. F., Weissman, J. S., & Huang, B. (2016a). Versatile protein tagging in cells with split fluorescent protein. *Nature Communications*, *7*, 1–9. https://doi.org/10.1038/ncomms11046
- Kamiyama, D., Sekine, S., Barsi-Rhyne, B., Hu, J., Chen, B., Gilbert, L. A., Ishikawa, H., Leonetti, M. D., Marshall, W. F., Weissman, J. S., & Huang, B. (2016b). Versatile protein tagging in cells with split fluorescent protein. *Nature Communications*, 7, 11046. https://doi.org/10.1038/ncomms11046
- Khan, M. (2017). Molecular engineering of plant development using Agrobacterium-mediated protein translocation. *Leiden University, Thesis*, 1–129.
- Kosugi, S., Hasebe, M., Matsumura, N., Takashima, H., Miyamoto-Sato, E., Tomita, M., & Yanagawa, H. (2009). Six classes of nuclear localization signals specific to different binding grooves of importinα. *Journal of Biological Chemistry*, 284(1), 478–485. https://doi.org/10.1074/jbc.M807017200
- Laboratories, B. R. (1986). BRL pUC host: E. coli DH5α competent cells. Focus, 8(2), 9.
- Lim, H. N., Lee, Y., & Hussein, R. (2011). Fundamental relationship between operon organization and gene expression. *Proceedings of the National Academy of Sciences*, 108(26), 10626–10631. https://doi.org/10.1073/pnas.1105692108
- Lowe, K., Wu, E., Wang, N., Hoerster, G., Hastings, C., Cho, M.-J., Scelonge, C., Lenderts, B., Chamberlin, M., Cushatt, J., Wang, L., Ryan, L., Khan, T., Chow-Yiu, J., Hua, W., Yu, M., Banh, J., Bao, Z., Brink, K., ... Gordon-Kamm, W. (2016). Morphogenic Regulators *Baby boom* and *Wuschel* Improve Monocot Transformation. *The Plant Cell*, *28*(9), 1998–2015. https://doi.org/10.1105/tpc.16.00124
- Mangano, S., Gonzalez, C. D., & Petruccelli, S. (1998). Arabidopsis Protocols. *Arabidopsis Protocols*, 1062, 165–173. https://doi.org/10.1385/0896033910

- Murashige, T., & Skoog, F. (1962). A Revised Medium for Rapid Growth and Bio Assays with Tobacco Tissue Cultures. 15.
- Nester, E. W. (2015). Agrobacterium: natureâ€TMs genetic engineer. *Frontiers in Plant Science*, 5(January), 1–16. https://doi.org/10.3389/fpls.2014.00730
- Nguyen, H. B., Hung, L. W., Yeates, T. O., Terwilliger, T. C., & Waldo, G. S. (2013). Split green fluorescent protein as a modular binding partner for protein crystallization. *Acta Crystallographica Section D: Biological Crystallography*, 69(12), 2513–2523. https://doi.org/10.1107/S0907444913024608
- Ostergaard, L., Abelskov, A. K., Mattsson, O., & Welinder, K. G. (1996). *Arabidopsis thaliana cell suspension culture*. *398*, 243–247.
- Pang, S. Z., DeBoer, D. L., Wan, Y., Ye, G., Layton, J. G., Neher, M. K., Armstrong, C. L., Fry, J. E., Hinchee, M. a, & Fromm, M. E. (1996). An improved green fluorescent protein gene as a vital marker in plants. *Plant Physiology*, *112*(3), 893–900. https://doi.org/10.1104/pp.112.3.893
- Park, E., Lee, H.-Y., Woo, J., Choi, D., & Dinesh-Kumar, S. P. (2017). Spatiotemporal Monitoring of *Pseudomonas syringae* Effectors via Type III Secretion Using Split Fluorescent Protein Fragments. *The Plant Cell*, *29*(7), 1571–1584. https://doi.org/10.1105/tpc.17.00047
- Pédelacq, J.-D., Cabantous, S., Tran, T., Terwilliger, T. C., & Waldo, G. S. (2006). Engineering and characterization of a superfolder green fluorescent protein. *Nature Biotechnology*, *24*(1), 79–88. https://doi.org/10.1038/nbt1172
- Pitzschke, A. (2013). Agrobacterium infection and plant defense-transformation success hangs by a thread. *Frontiers in Plant Science*, 4(DEC), 1–12. https://doi.org/10.3389/fpls.2013.00519
- Puigbò, P., Guzmán, E., Romeu, A., & Garcia-Vallvé, S. (2007). OPTIMIZER: A web server for optimizing the codon usage of DNA sequences. *Nucleic Acids Research*, *35*(SUPPL.2), 126–131. https://doi.org/10.1093/nar/gkm219
- Sakalis, P. A., van Heusden, G. P. H., & Hooykaas, P. J. J. (2014a). Visualization of VirE2 protein translocation by the Agrobacterium type IV secretion system into host cells. *MicrobiologyOpen*, 3(1), 104–117. https://doi.org/10.1002/mbo3.152
- Sakalis, P. A., van Heusden, G. P. H., & Hooykaas, P. J. J. (2014b). Visualization of VirE2 protein translocation by the Agrobacterium type IV secretion system into host cells. *MicrobiologyOpen*, 3(1), 104–117. https://doi.org/10.1002/mbo3.152
- Schneider, C. A., Rasband, W. S., & Eliceiri, K. W. (2012). NIH Image to ImageJ: 25 years of image analysis. *Nature Methods*, *9*(7), 671–675. https://doi.org/10.1038/nmeth.2089
- Shine, J., & Dalgarno, L. (1974). The 3' terminal sequence of Escherichia coli 16S ribosomal RNA: complementarity to nonsense triplets and ribosome binding sites. *Proceedings of the National Academy of Sciences of the United States of America*, 71(4), 1342–1346. https://doi.org/10.1073/pnas.71.4.1342

- Shultzaberger, R. K., Bucheimer, R. E., Rudd, K. E., & Schneider, T. D. (2001). Anatomy of Escherichia coli ribosome binding sites. *Journal of Molecular Biology*, 313(1), 215–228. https://doi.org/10.1006/jmbi.2001.5040
- Vergunst, A. C., Schrammeijer, B., den Dulk-Ras, A., de Vlaam, C. M. T., Regensburg-Tuïnk, T. J. G., & Hooykaas, P. J. J. (2000). VirB/D4-Dependent Protein Translocation from Agrobacterium into Plant Cells. *Science*, *290*(5493), 979–982. https://doi.org/10.1126/science.290.5493.979
- Wroblewski, T., Tomczak, A., & Michelmore, R. (2005). Optimization of Agrobacterium-mediated transient assays of gene expression in lettuce, tomato and Arabidopsis. *Plant Biotechnology Journal*, *3*(2), 259–273. https://doi.org/10.1111/j.1467-7652.2005.00123.x
- Zhang, Y., Chen, M., Siemiatkowska, B., Toleco, M. R., Jing, Y., Strotmann, V., Zhang, J., Stahl, Y., & Fernie, A. R. (2020). A Highly Efficient Agrobacterium-Mediated Method for Transient Gene Expression and Functional Studies in Multiple Plant Species. *Plant Communications*, 1(5), 100028. https://doi.org/10.1016/j.xplc.2020.100028